signals are fed into the optical coupler and divided into the N delay lines, which have the relative delay time of $k\Delta t$. After shifting the phase of the delayed signals by $2\pi nk/N$, the signals are added by the coupler and correlated with each other. Operation in the time domain is also needed because the orthognality holds within one bit; that is, the optical DFT is effective for the duration of unchanged $d_n(t)$. Therefore, we need to synchronize the incoming bit streams at the input, and to place an optical gate that extracts the duration of T/N, where the same bits are overlapped at the output. Note that it is not necessary to synchronize the phase of the input light in this time domain operation.

The proposed scheme can separate the substantially overlapped spectrum, whereas overlapping of the spectrum is not permitted in conventional optical filter separation. And it is possible to achieve the spectral efficiency up to 1 bit/s/Hz in principle.

3. Experiment results

We experimentally demonstrated separation of one signal from three multiplexed signals by using the scheme. Fig. 2 schematically shows the experimental setup. We used DFB lasers as light sources. The frequency difference of the DFB lasers was set to 6.25 GHz. One $LiNbO_3$ modulators modulated the center and another modulated both sides of the lights at 5 Gb/s with NRZ format. And the signals were multiplexed by an optical coupler with the same polarization. In this case, the spectral efficiency reached 0.8 bit/s/Hz. We used a PLC Mach-Zehnder interferometer (MZI) for separation. It functions as the optical delay lines, the phase shifter, and the coupler in this case. The free spectral range was 12.5 GHz and the corresponding delay time was 80 ps. The phase shift condition was satisfied because the phase difference between the two output ports was π. An electroabsorption (EA) modulator was used as the optical gate. The modulator was driven at a 5-GHz clock to extract the effective time range.

The observed optical spectra and the eye patterns at different stages are also shown in Fig. 2. The solid lines denote the spectra of the multiplexed signal, and the dotted lines are spectra of only one signal. As shown in Fig. 2(a), the spectra overlapped considerably and no eye opening was observed due to the beating between signals, which occurred because the frequency differences between neighboring channels were close to the bandwidth of the optical receiver, which is known as coherent clostalk. Fig. 2(b) shows the eye pattern after the signal passed through the MZI. The eye opening was observed only when the same bit was overlapped after propagating through the two delay lines of the MZI. And no eye opening due to the beating was observed at other times. This shows the signal was separated within the limited time slot as described in the principle. Fig. 2(c) shows the eye pattern after the region where the eye opened was extracted by the EA modulator. Only a clearly opened eye pattern was observed. Furthermore, in the spectrum, the demultiplexed spectrum completely agreed with the spectrum obtained without neighboring signals in the modulation bandwidth range. This shows that this scheme can completely separate one modulated spectrum from the substantially overlapped other signal without coherent crosstalk.

To estimate the quality of the separation of the center signal with this scheme, we measured the bit error rate (BER) performances after the optical gate. Fig. 3 shows the BERs versus the received power after separating one signal from two or three multiplexed signals. Error-free separation was achieved and the power penalty at the BER = 10^{-9} was about 3 dB, even in the case of the separation from the three signals. The power penalty arises due to the coherent crosstalk resulting in the imperfectness of the MZI. The origin of the observed error floor may be frequency chirp caused by the $LiNbO_3$ modulator, which may be removed by using a dual-electrode-type chirp-free modulator. Furthermore, the number of multiplexed wavelengths could be extended easily because the multiplexed signals far from neighbors contribute to the power penalty as incoherent crosstalk rather than as coherent crosstalk, which is the same condition as the conventional WDM systems.

4. Summary

We have proposed a novel optical orthogonal frequency division multiplexing technique that can overcome the spectral efficiency limitation of the conventional WDM system. This scheme permits substantial overlapping of the spectrum and can achieve the spectral efficiency up to 1 bit/s/Hz in principle. For demultiplxing, we used a newly developed optical DFT instead of electrical digital processing, which is impossible to apply in the optical frequency range. The optical DFT was realized by using a set of delay lines, a phase shifter and a coupler in the frequency domain and bit synchronization and an optical gate in the time domain. In experimental demonstration of this scheme, error-free operation was obtained with a 0.8 bit/s/Hz of spectral efficiency.

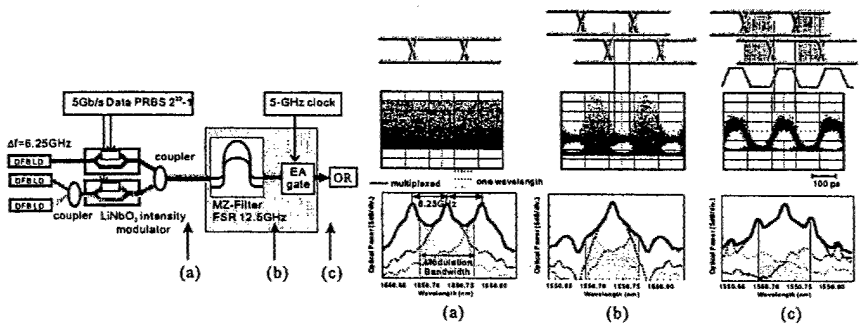

ThD1 Fig. 2. Experimental setup and eye pattern and optical spectra of signals at different stages. (a) Before MZI, (b) after MZI, (c) after EA gate.

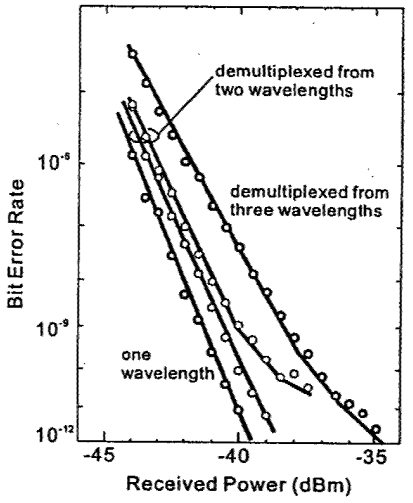

ThD1 Fig. 3. Bit error rate of the demultiplexed signals.

References

1. Y. Yano, T Ono, K. Fukuchi, T. Ito, H. Yamazaki, M. Yamaguchi and K. Emura, "2.6 Terabit/s WDM Transmission Experiment using Optical Duobinary Coding," in ECOC '96, Oslo, 1996, ThB. 3. 1.
2. Y. Idler, S. Bigo, Y. Frignac, B. Franz and G. Veith, "Vestigial Side Band Demultiplexing for Ultra High Capacity (0.64 bit/s/Hz) Transmission of 128 × 40 Gb/s Channels," in OFC 2001, Anaheim, 2001, MM 3-2.
3. T. Miyakawa, I. Morita, K. Tanaka, H. Sakata and N. Edagawa, "2.56 Tbit/s (40 Gbit/s × 64 WDM) Unrepeated 230 km Transmission with 0.8 bit/s/Hz Spectral Efficiency Using Low-Noise Fiber Raman Amplifier and 170 μm^2-A_{eff} Fiber," in OFC 2001, Anaheim, 2001, PD 26-1.
4. For example, L.J. Cimini, Jr., "Analysis and Simulation of a Digital Mobile Channel Using Orthogonal Frequency Division Multiplexing," IEEE Trans. Commun., COM-33, pp. 665–675 (1985).

ThD2 **9:30 am**

2.5 Gb/s Chaotic Optical Communication

S. Tang and J.M. Liu, *Department of Electrical Engineering, University of California, Los Angeles, Los Angeles, CA 90095-1594, Email: tangs@ee.ucla.edu*

Chaotic communication has recently attracted great interests because of its potential applications in secure communications and spread spectrum communications. In a chaotic communication system, chaotic output from a transmitter is used as carrier waveform to encode a message. The chaotic waveform is noise-like in time series and broadband in spectrum. Therefore, the massage can be hidden by the chaotic waveform in both time and frequency domains. To recovery the message, a replica of the chaotic carrier has to be reproduced at the receiver side, which is achieved through chaos synchronization. Theory of chaos synchronization indicates that two identical systems can be synchronized in chaotic states if they are parameter-matched and are driven by a common force. Message decoding is then

achieved by removing the chaotic carrier from the received signal at the receiver. On the other hand, eavesdroppers cannot recover the message because of the lack of information about the parameters.

Chaotic communication has been investigated using electric circuits, which are generally bandwidth-limited to the kilohertz region. To achieve fast chaotic communication, laser systems are of great interests because of the potential improvement of bandwidths to the gigahertz region. Different laser systems have been investigated in chaotic optical communications. Chaotic optical communication systems using semiconductor lasers with optical feedback have been investigated and the transmission of a square wave at a frequency of 9.5 kHz has been reported.[1] With fiber-ring lasers, high-speed chaotic optical communication has been demonstrated to transmit a digital signal at 250 Mb/s[2] and a sinusoidal signal at 1 GHz.[3] Because of the wide application of semiconductor lasers in optical communications, investigations on fast chaotic optical communication systems using semiconductor lasers are of great importance. In this paper, we report our experimental results of 2.5 Gb/s chaotic optical communication using fast chaotic pulsing semiconductor lasers. The 2.5 Gb/s bit-rate is the highest among the reported experiments about chaotic communication. This experiment demonstrates that chaotic communication at commercial bit-rate standard is achievable.

The schematic of the chaotic communication system using chaotic pulsing semiconductor lasers is shown in Fig. 1. The fast chaotic pulsing is generated by a semiconductor laser operated in a highly nonlinear region with delayed optoelectronic feedback. The chaotic pulsing has both chaoticly varying pulse intensity and pulse interval. In the setup, the transmitter laser has an optoelectronic feedback loop which drives the laser into chaotic pulsing at certain delay times through a route of quasiperiodicity.[4] The message $m(t)$ is encoded by additive chaos modulation as $S^T(t) + m(t)$ after the light comes out of the transmitter laser, with $S^T(t)$ the chaotic output of the transmitter. On the receiver side, a receiver laser is driven by $S^T(t) + m(t)$, which is the same force that drives the transmitter laser. When the two lasers are parameter-matched, they can synchronize and the receiver laser can reproduce the chaotic pulsing output of the transmitter laser as $S^R(t) = S^T(t)$. The message is recovered by subtracting the reproduced chaotic waveform at the output of the receiver laser from the received signal through an inverter and a combiner as $S^T(t) + m(t) - S^R(t) = m(t)$.

In the experiment, the two lasers are identical InGaAsP/InP single-mode DFB lasers with wavelengths at 1.299 μm. Both lasers are temperature stabilized at 21.00°C. The photodetectors are InGaAs photodetectors (6 GHz bandwidth), and the amplifiers are Avantek SSF86 amplifiers (0.4–3 GHz bandpass). The 2.5 Gb/s message is $2^{10} - 1$ pseudorandom NRZ signal generated by an HP 70843A pseudorandom pattern generator. The optical output time series detected by the photodetectors are observed with a Tektronix TDS 694C digital real-time oscilloscope with a 3 GHz bandwidth and an up to 1×10^{10} Samples/sec sampling rate. The eye patterns are measured with a Tektronix TDS 8000 digital sampling oscilloscope.

Figure 2 shows the experimental results of the transmission of the 2.5 Gb/s NRZ digital signal through the chaotic communication system. The time series and the eye pattern of the received signal, $S^T(t) + m(t)$, before the subtraction of the chaotic carrier, are shown in Figs. 2(a). In the received signal, $m(t)$ is encoded by the chaotic pulsing carrier $S^T(t)$ generated by the transmitter laser. Because of the noise-like nature of the chaotic carrier, the message is hidden by the carrier waveform and direct detection is impossible. In the eye pattern, the eyes are almost closed and very noisy. To recover the message, chaos synchronization has to be achieved between the transmitter and the receiver lasers, which requires that the two lasers be parameter-matched and driven by a common force. Parameter-matching is a key to the security of the chaotic system. The parameters of the components of the transmitter and the receiver have to be matched respectively. Since the semiconductor lasers are nonlinear devices which are operated in a highly-nonlinear region of chaotic pulsing, the match of the internal laser parameters are very demanding. In the experiment, the two lasers are carefully chosen from the same batch which have the closest characteristics and their operating conditions are also fine tuned. In Ref.[5], high quality of chaos synchronization in our system has been reported and the correlation coefficient between the outputs of the transmitter and the receiver was found to be as high as 0.95. Using the inverter and the combiner in the setup, the message is recovered by subtracting the chaotic carrier from the received signal, which is shown in Figs. 2(b). The time series now clearly shows the pattern of the message after the noise-like carrier is subtracted. In the eye pattern, the eye opening is much improved compared with that in Figs. 2(a). A threshold can be placed within the clear area of the eyes and reliable detection can be achieved. The high quality of message recovery in our experiment is demonstrated by comparing the results in Figs. 2(b) with those in Figs. 2(c) which are the results of the message passed through the same channel path but without the use of chaotic carrier. We can see that there is not much deterioration of the message recovery after chaotic communication technology is launched. Because of the problems of impedance match and speed limitation from the components, the message is already distorted before any chaotic communication technology is applied. Therefore, after the improvement of those problems, the performance of the chaotic system can be much improved.

The challenge in a chaotic communication system is to reach reliable chaos synchronization between the transmitter and the receiver. Deviation from perfect parameter-match creates syn-

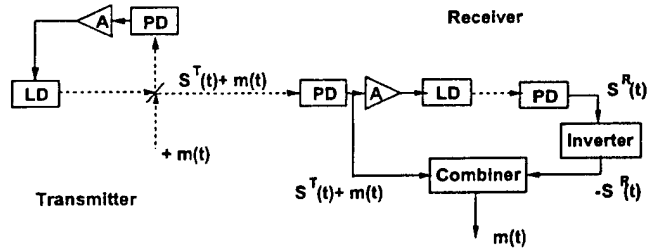

ThD2 Fig. 1. Schematic of the chaotic communication system with chaotic pulsing semiconductor lasers. LDs: Laser Diodes, PDs: Photodetectors, As: Amplifiers.

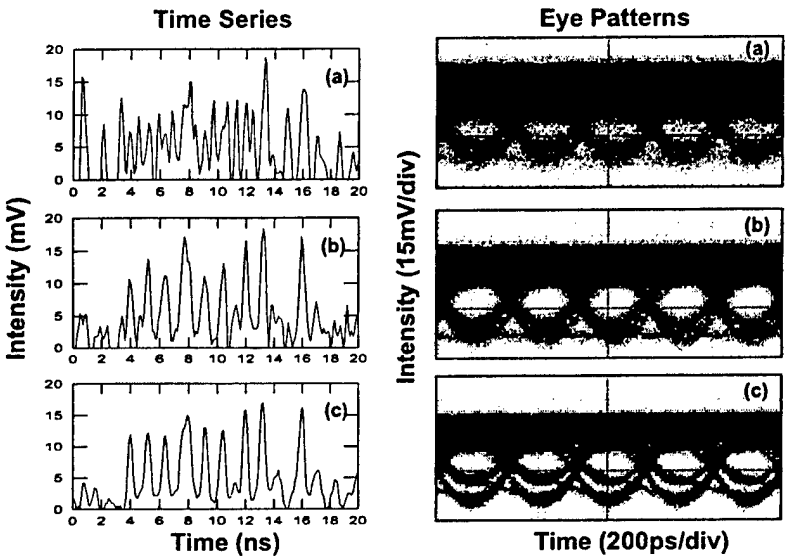

ThD2 Fig. 2. Message recovery of the 2.5 Gb/s chaotic optical communication system. (a) Received signal before the subtraction of the chaotic carrier. (b) Recovered message after the subtraction of the chaotic carrier. (c) Received message without the use of chaotic carrier.

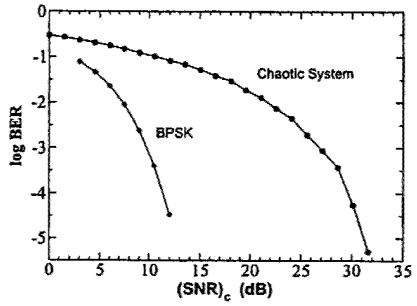

ThD2 Fig. 3. Theoretical calculation of BER vs. $(SNR)_c$ of the chaotic optoelectronic feedback system. The BER of a BPSK system is also shown for comparison.

chronization error in the system. Channel noise and intrinsic laser noise are also sources of synchronization errors. Theoretical performance calculation of the chaotic communication system with chaotic pulsing semiconductor lasers is demonstrated in Fig. 3 where BER is plotted as a function of the signal-to-noise-ratio in the channel $(SNR)_c$ when channel noise exists. In comparison, a traditional BPSK system is also shown. A power penalty of 19 dB is observed for the chaotic communication system compared with the traditional BPSK system. To improve the performance of a chaotic communication system, it is important to improve the synchronization quality and also improve the robustness of the system to the influence of noise.

In conclusion, digital signal at 2.5 Gb/s bit-rate has been successfully transmitted in a chaotic communication system. The communication quality and capacity are both shown to be very high with this chaotic pulsing semiconductor laser system, which indicates that chaotic communication with several Gb/s bit-rate is feasible with semiconductor lasers.

References

1. S. Sivaprakasam and K.A. Shore, "Message encoding and decoding using chaotic external-cavity diode lasers," *IEEE J. Quantum Electron.* 36, 35–39 (2000).
2. G.D. VanWiggeren and R. Roy, "Chaotic communication using time-delayed optical systems," *Int. J. Bifurcation and Chaos* 9, 2129–2156 (1999).
3. L.G. Luo, P.L. Chu, and H.F. Liu, "1 GHz optical communication system using chaos in erbium-doped fiber lasers," *IEEE Photon. Tech. Lett.* 12, 269–271 (2000).
4. S. Tang and J.M. Liu, "Chaotic pulsing and quasiperiodic route to chaos in a semiconductor laser with delayed optoelectronic feedback" *IEEE J. Quantum Electron.* 37, 329–336 (2001).
5. S. Tang and J.M. Liu, "Synchronization of high-frequency chaotic optical pulses," *Opt. Lett.* 26, 596–598 (2001).

ThD3 **(Invited)** **9:45 am**

High-capacity DWDM/ETDM transmission

Joerg-Peter Elbers, *Marconi Communications ONDATA GmbH, Gerberstr. 33, D-71522 Backnang, Germany, Email: joerg-peter.elbers@marconi.com*

1. Introduction

High-capacity, terrestrial optical transmission systems are now being widely deployed offering aggregate capacities >1 Tb/s over distances of >1,000 km. They use dense wavelength-division multiplexing (DWDM) techniques in combination with high-speed electrical time-division multiplexing (ETDM) to minimize the cost per bit and kilometre whilst maintaining flexibility and scalability at the same time.

This paper reviews the current state-of-the-art of high-capacity, terrestrial DWDM/ETDM systems in research and development. It explains design rules and limitations fundamental to these systems and discusses challenges and enabling technologies for next-generation optical networks employing transparent photonic switching.

2. State-of-the art in research and development

Most commercial Tb/s-DWDM systems operate with >100 channels at 10 Gb/s line rate using a channel spacing of 50 GHz in both the C- and L-band of the Erbium-doped amplifiers (EDFAs). To achieve a sufficiently high optical signal-to-noise ratio (OSNR) at the receiver site and to meet the target reach of the system, a forward error correction (FEC) scheme with a (255,239)-Reed-Solomon code (according to ITU-T G.709) is used, reducing the required OSNR (typically in the range of 23 dB in 0.1 nm optical bandwidth for non-return to zero (NRZ) systems and a BER $<10^{-15}$) by approximately 6 dB. Raman amplification can be employed additionally to maintain large span losses typically present in terrestrial systems with span lengths in the range of 80..100 km. Depending on the number of channels present, a reach of several thousand km can be achieved.[1]

40 Gb/s line rate is already at an advanced prototype stage and is extensively used for multi-Tb/s laboratory and field demonstrations. With a gap between the first laboratory experiments and the market introduction of commercial products of approximately 2–3 years, it is expected that the first 40 Gb/s solutions with 100 GHz channel spacing will appear on the market somewhere around next year. As for 10 Gb/s, the expected cost savings lead to realizations of 40 Gb/s transmitters and receivers with high-speed electronics instead of optical time division multiplexing, albeit the sensitivity of 40 Gb/s-ETDM receivers is still some dB worse in comparison to ODTM devices due to the current maturity of high-speed SiGe technology. FEC is a prerequisite for 40 Gb/s systems to obtain a sufficiently high performance. Raman amplification again helps to maintain large span lengths of typical terrestrial transmission systems.

Recently, more than 10 Tb/s aggregate capacity on a single fibre was demonstrated in a laboratory experiment;[2,3] 3.2 Tb/s were transmitted in a successful field trial over an installed fibre link.[4] Whilst the aggregate capacity is growing fast over the last years, the capacity-length-product actually exhibits a much lower growth rate.

Comparing configurations with 10 and 40 Gb/s per channel, 40 Gb/s line rates offers multi-Tb/s aggregate capacities and spectral efficiencies not achievable with current 10 Gb/s technology. 10 Gb/s, in contrast, allow for a longer system reach. From these observations, 40 Gb/s transmission is more suited for "short fat pipe" applications, where large capacities have to be transported economically between two 3R-regeneration sites spaced several 100 km apart, whereas 10 Gb/s is the candidate of choice for ultra long-haul transmission on installed fiber and the enabler for regenerator-free ultra-long distance transmission and all-optical networking.

Commercial systems and most lab experiments are based on NRZ and return to zero coding (RZ) schemes. Advanced modulation formats such as duobinary coding or single/vestigial sideband transmission (SSB/VSB) are used to increase the overall capacity by increasing the spectral efficiency. However, this increase is often associated with a reduction in receiver sensitivity and hence a reduction in the overall system reach.[5] Additionally, the system design is typically more complex. Another option for increased spectral efficiency is a reduction in the DWDM channel spacing. However, the maximum reach is also reduced as linear and nonlinear channel-channel-interaction effects are more pronounced.

Other means to increase the aggregate system capacity include the use of new amplifier bands, namely the S-band,[6] for which amplifiers are now commercially available. The deployment of S-band amplifiers is heavily dependent on both economic and technical constraints. Fiber shortage is not an issue in most core networks, and an evaluation must be made of the trade-off between lightening an extra fiber and accepting the inevitable transmission penalty arising from band-band interactions.

Special fiber types (very large effective area fiber, reverse dispersion fiber), optimized dispersion maps and shorter amplifier spans are commonly employed in ultra-long haul submarine systems,[7] and recently terrestrial systems started borrowing these techniques from the submarine world.[8] Whereas the first two options help to carefully manage signal distortions and signal impairments associated with nonlinear fiber transmission, the shorter amplifier spacing leads to a lower span loss and a higher system reach in any case (e.g., a reduction of the span length by one half doubles the system reach in a noise-limited system and increases the reach by a factor of 1.4 in a system limited by nonlinear impairments). Since the fiber type and span length is already fixed in existing terrestrial networks, such approaches are more suited for (future) greenfield installations. The system design in this case is based on a cost trade-off between more multi-channel EDFAs (albeit lower power) and additional regenerator sites.

3. System design and limitations

Whilst DWDM systems are digital transmission systems operating on binary input and output data, the optical fiber transmission medium is analog in nature and requires careful system design to guarantee an optimum system performance. In linear terms, the performance is mainly degraded by optical noise. Most important nonlinear limitations are the fiber effects self-phase modulation (SPM), cross-phase modulation